

UV-activated room temperature single-sheet ZnO gas sensor

Fanli Meng¹ ✉, Hanxiong Zheng², Yufeng Sun² ✉, Minqiang Li³, Jinhuai Liu³

¹College of Information Science and Engineering, Northeastern University, Shenyang 110819, People's Republic of China

²Department of Mechanical and Automotive Engineering, Anhui Polytechnic University, Wuhu 241000, People's Republic of China

³Nanomaterials and Environment Detection Laboratory, Institute of Intelligent Machines, Chinese Academy of Sciences, Hefei 230026, People's Republic of China

✉ E-mail: mengfanli@ise.neu.edu.cn, sunyufeng118@126.com

Published in Micro & Nano Letters; Received on 8th March 2017; Revised on 25th May 2017; Accepted on 15th June 2017

Room temperature sensor is a research hot for metal–oxide gas sensors. However, electron activation is a bottleneck to improve sensitivity for room temperature sensors. Here, an ultraviolet (UV)-activated gas sensor based on a single-sheet porous single-crystalline (PSC) zinc oxide (ZnO) sheet has been fabricated instead of heating activation, which works at room temperature. The PSC ZnO nanosheets were first prepared by a one-pot wet-chemical method. Then, the precursors were annealed for 2 h in air to obtain the PSC ZnO nanosheets. They were characterised by scanning electron microscopy, high-resolution transmission electron microscopy and UV–visible spectrum. Finally, the single-sheet ZnO gas sensors were fabricated by focused ion beam technology, which exhibited good responses to 1–300 ppm of ethanol. The single-sheet ZnO UV-activated sensing mechanism was also put forward to explain the excellent sensing property.

1. Introduction: Metal–oxides have been extensively used as gas sensors because they have lots of advantages [1–3]. Especially, various nanostructures have been developed to improve their gas-sensing properties [4, 5]. Zinc oxide (ZnO), as a popular gas-sensing material, has been prepared to many nanostructured gas sensors such as nanorods [6], nanowires [7], nanosheets [8] and hierarchical structures [9–11] have been used as gas-sensing materials. For example, Liang *et al.* exploited ZnO nanorods and nanosheets to fabricate gas sensors to detect nitrogen dioxide (NO₂) and acetone [12–16]. However, most of metal–oxide-based gas sensors need heating to activate the separation of electron–hole to form charge depletion layer on the surfaces of metal–oxides, which not only increase power consumption but also is dangerous for inflammable and explosive gas detection.

Nanostructured materials have shown great promise for developing room temperature gas sensors [17, 18]. Instead of heating activation, ultraviolet (UV)-activated ZnO gas sensors have recently been developed, which can also work at room temperature [19–22]. However, it has been reported that polycrystalline structures make gas sensor loss stability, and therefore porous single-crystalline (PSC) ZnO nanosheets have been developed, which exhibited significantly long-term stability as well as highly sensitive performance [23]. Sheet-like semiconductors were expediently utilised to fabricate room temperature gas sensors activated by light [24, 25]. Here, a single-sheet PSC ZnO nanosheet-based gas sensor has been fabricated, which can be activated by UV light and work at room temperature.

2. Experimental results: The PSC ZnO nanosheets were first prepared by a one-pot wet-chemical method as our previous reports [26, 27]. Typical procedure is as follows: Zn acetate (1 g) and urea (3 g) were first dissolved into deionised water (40 ml) and then the solution was stirred for 30 min. After that, it was sealed in a conical flask and then put into an oven under 100°C for 4 h. When the solution was cooled down, the precipitate was centrifuged and washed several times. Then, it was dried at 60°C. Finally, the precursors were annealed at 300°C for 2 h in air to obtain the PSC ZnO nanosheets.

The PSC ZnO nanosheets were then fabricated to a single-sheet ZnO gas sensor: first, a pair of interdigital electrodes (IDEs) was fabricated on silicon (Si)/Si dioxide (SiO₂) substrate by lift-off

process. The gap between the electrodes is about 20 µm. The electrodes were deposited by 30 nm titanium and 50 nm gold (Au). The synthesised PSC ZnO nanosheets were collected and dispersed in ethanol. Then, the nanosheet-suspended ethanol was dropped onto the Si/SiO₂ substrate equipped with IDEs. In this way, the PSC ZnO nanosheets were dispersed between the pair of IDEs. At last, a single-sheet PSC ZnO nanosheet was selected to deposit a pair of platinum (Pt) layers connected to the IDEs by focused ion beam (FIB) to form electric connection.

Typically, a closed test chamber (~1000 ml) was used to perform gas-sensing measurement, in which an inlet and an outlet were equipped for gas flow. The gas sensors were connected to a Keithley 6487 source/measure unit (SMU) to record the current signals as well as to provide a power source. A 9 W 365 nm UV lamp was placed on the top of the device (~6 mW/cm²) to measure the gas-sensing properties of the sensors under UV radiation. Typically, a gas-sensing test was done as follows: the target gas (e.g. ethanol) was first introduced into the test chamber by extracting the headspace of the liquid samples at room temperature using a microsyringe. The concentration of the target gas could be calculated by the saturated vapour pressure of the organic vapour samples under a standard atmospheric pressure. Then, the UV lamp was periodically turned on and off. The current signals were measured and acquired by SMU under a constant voltage (5 V) between the pair of electrodes of the single-nanosheet PSC ZnO. Finally, fresh synthesised air was introduced into the testing chamber to release target gases once the gas-sensing measurement was over.

The response of the sensor is defined as

$$\text{response} = \frac{I_g - I_a}{I_a} \times 100\% \quad (1)$$

Here, I_a and I_g are the currents of the sensor under UV light irradiation in air and target gas, respectively.

3. Results and discussion: The morphologies of the as-prepared products were characterised by TEM (Fig. 1), high-resolution transmission electron microscopy (HRTEM) (Fig. 2) and UV–visible (UV–vis) spectrum (Fig. 3). From the TEM image, the porous structure of the ZnO nanosheet can be observed. From the

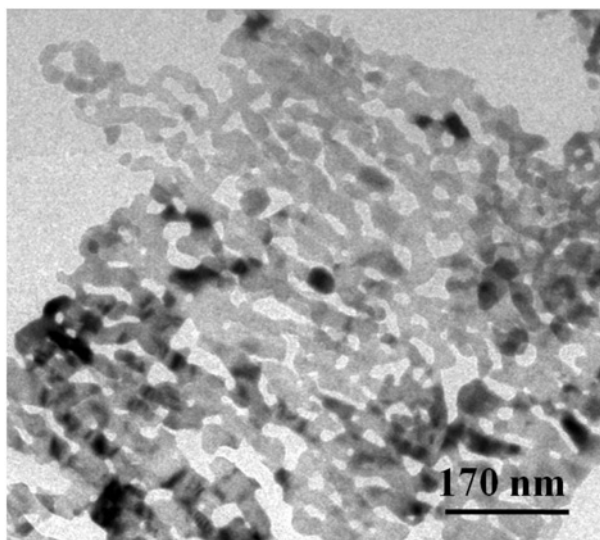


Fig. 1 TEM image of the PSC ZnO nanosheet

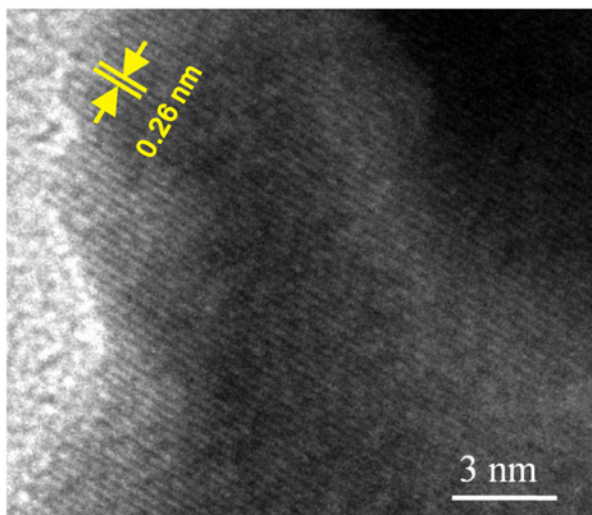


Fig. 2 HRTEM image of the PSC ZnO nanosheet

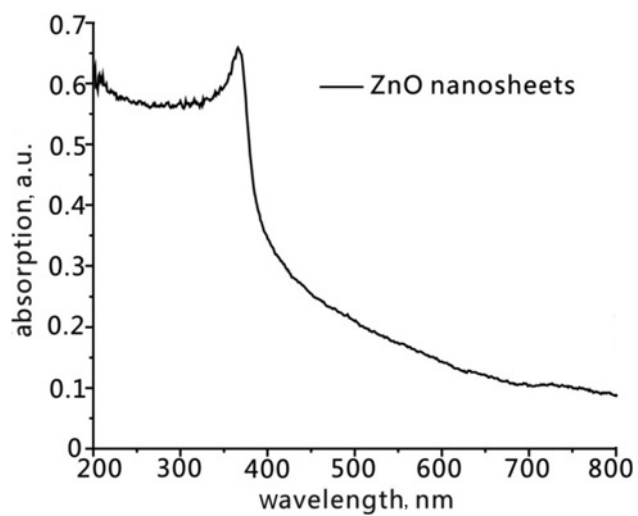


Fig. 3 UV-vis spectrum of the PSC ZnO nanosheets

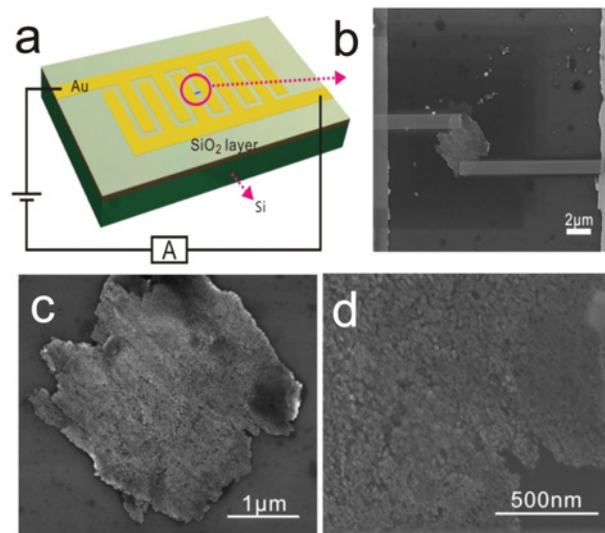


Fig. 4 Schematic diagram of the sensor structure
a Schematic diagram of the sensor structure
b SEM image of the PSC ZnO nanosheet connected to IDEs by Pt strip
c, d SEM images of the PSC ZnO nanosheet

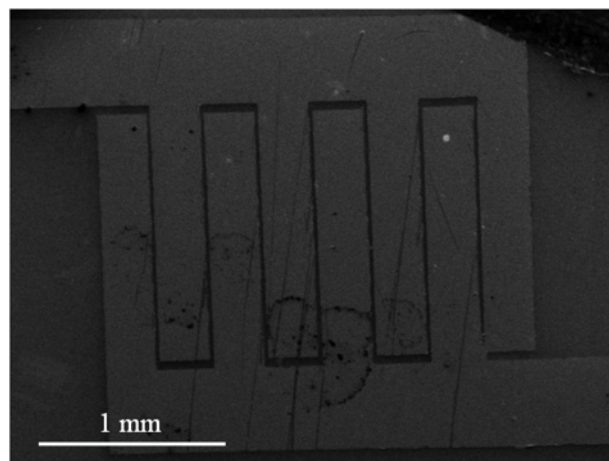


Fig. 5 SEM image of the IDEs

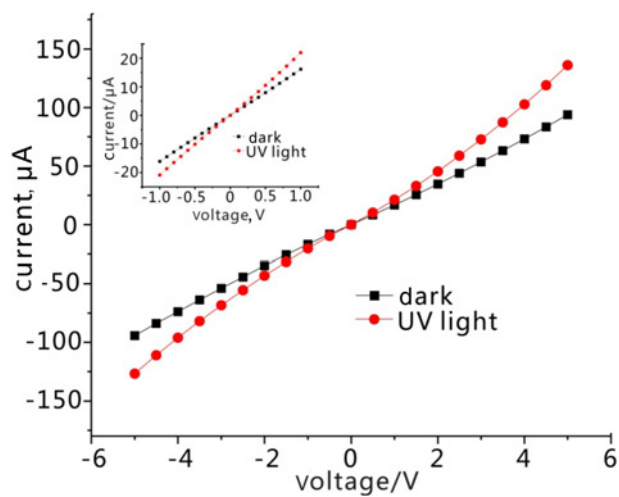


Fig. 6 I-V curves of the sensor measured in air

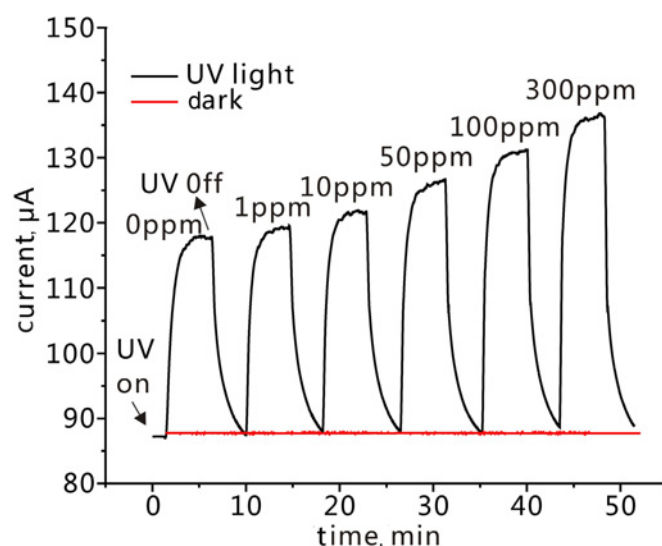


Fig. 7 Responses of the sensor to different concentrations of ethanol under the UV light

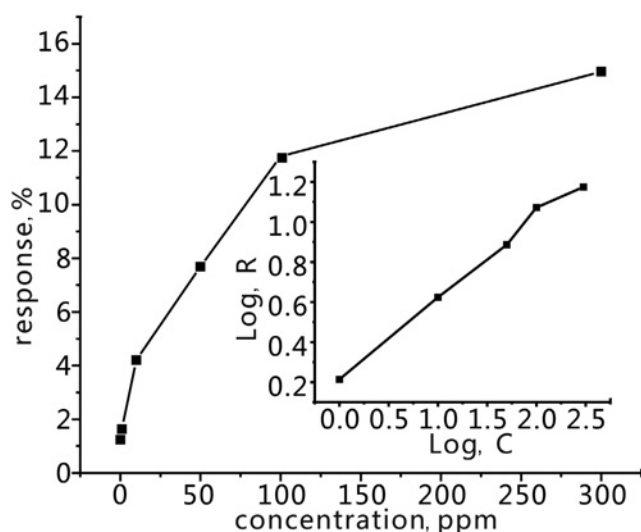


Fig. 8 Plot of the response versus gas concentration obtained from Fig. 7. The inset is the relationship between $\log(R)$ and $\log(C)$

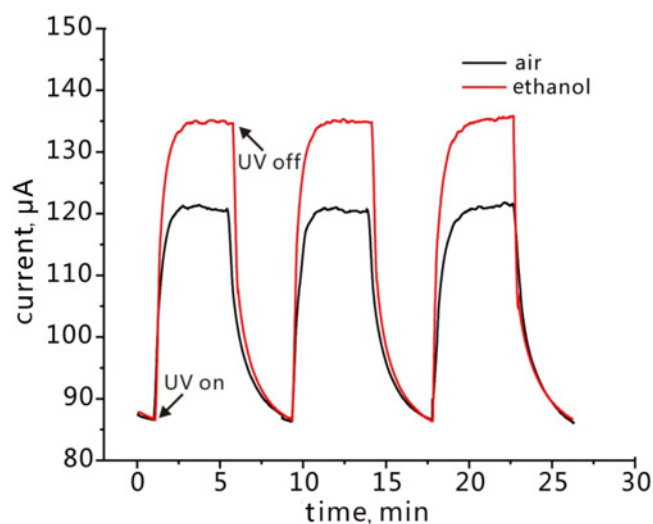


Fig. 9 Responses of the sensor under the UV light in air and in 300 ppm of ethanol

HRTEM image, it can be clearly seen that many coherent lattice fringes cover the whole nanosheet. The lattice spacing of 0.26 nm is indexed to the (002) planes of the hexagonal phase of ZnO. Therefore, it can be confirmed that the ZnO nanosheet is a SC structure. UV-vis spectrum was exploited to characterise the UV adsorption properties of the PSC ZnO nanosheets. A peak around 365 nm is observed which could reveal the UV response property of the PSC ZnO nanosheets. Therefore, UV light may activate the separation of electron-hole to form charge depletion layer on the surfaces of ZnO.

The schematic diagram of the sensor structure is shown in Fig. 4a, in which a piece of PSC ZnO nanosheet is connected to Au IDEs.

Fig. 4b shows the scanning electron microscopy (SEM) images of the PSC ZnO nanosheet connected to IDEs by Pt strip, from which it can be seen that the ZnO nanosheet is about $3 \times 3 \mu\text{m}^2$ and the Pt strip is about $1 \mu\text{m}$ in width. The high magnification SEM images are shown in Figs. 4c and d, from which the mesoporous structure can also be clearly seen. The porous and SC structure has also been characterised in our previous work [26, 27].

Fig. 5 shows the SEM image of the IDEs from which it can be seen that the gap between the electrodes is about $20 \mu\text{m}$. Fig. 6

shows the I - V curves of the device measured in air. The linear I - V response indicates the PSC ZnO nanosheet has a good ohmic contact to the electrodes, suggesting successfully deposition of Pt strip by FIB. Fig. 6 also reveals that the current obviously increases when the ZnO nanosheet is under UV irradiation, which could be attributed to the UV activation.

Fig. 7 shows the response curves of the sensor to different concentrations of ethanol under the UV light radiation at room temperature. The responses increase with the concentration change of ethanol from 1 to 300 ppm. When the UV light turns off, the response currents will recover to the baseline. The responses are higher than UV-activated room temperature sensors based on one-dimensional (1D) nanostructures [21, 22] because 2D nanostructures have more contact areas and the PSC structures provide more active sites. The response and recovery times of the sensor are 2 and 4 s, respectively, which are mostly same for different concentrations. Fig. 8 shows the plot of the response versus gas concentration obtained from Fig. 7. From the plot, it can be seen that the response increases sub-linearly, which may be caused by the falling down of the adsorption ability of the PSC ZnO nanosheet with increase of ethanol concentration. However, the relationship between $\log(R)$ and $\log(C)$ is linear as shown in the inset.

Table 1 Comparison of the gas-sensing performance of the UV-activated ZnO gas sensors

Materials	Target gases	Operating temperature	Detection range	References
polycrystalline ZnO film	H ₂	Room temperature (RT)	100 ppm	[20]
ZnO fibres	benzene, toluene, acetone, ethanol	RT	10–60 ppm	[21]
SnO ₂ @ZnO nanowires	NO ₂	RT	1–5 ppm	[22]
single ZnO sheet	ethanol	RT	1–300 ppm	this work

Bold values indicate the results discussed in this letter

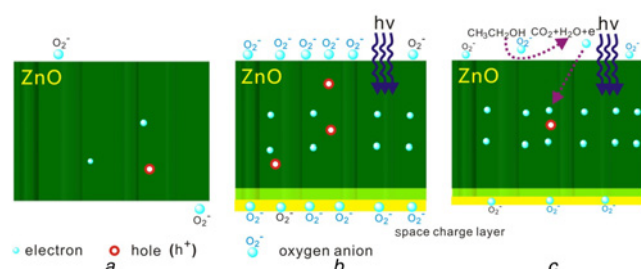


Fig. 10 Schematic illustration of the UV-activated sensing mechanism
 a the PSC ZnO nanosheets
 b the PSC ZnO nanosheets under UV-radiation
 c the reaction of ethanol on the surface of the PSC ZnO nanosheets under UV-radiation

The stability of the UV response of the PSC ZnO nanosheets was investigated by a three-cycle continuous measurement Fig. 9. From which it can be seen that the device is stable both in air and in ethanol, it can guarantee the gas-sensing response properties of the PSC ZnO nanosheets. Table 1 shows the comparison of the gas-sensing performance of the UV-activated ZnO gas sensors. From this table, it can be observed that all the ZnO gas sensors work at room temperature under UV activation. The single ZnO sheet sensor has the widest detection range which responds to ethanol in the range of 1–300 ppm. The lowest detection concentration of 1 ppm is also the lowest among the UV-activated ZnO gas sensors.

The UV-activated sensing mechanism of the PSC ZnO nanosheet is proposed as shown in Fig. 10. ZnO is an *n*-type semiconductor, in which electrons are charge carriers. Generally, there are a few mobile electrons at room temperature. The oxygen gases adsorbed on the surface of the ZnO sensing material in air can also capture only a few electrons (Fig. 10a). Under the irradiation of UV light, abundant electron–hole pairs separated and the electrons are trapped by oxygen gases to form negative oxygen anions (O₂[−]). These oxygen anions cause a depletion layer and thus a reduced surface conductivity (Fig. 10b). When ethanol molecules are introduced, they will react with oxygen anions and the electrons trapped by the oxygen anions will return to the ZnO nanosheet. Therefore, the depth of depletion layer will decrease and thus the surface conductivity will increase (Fig. 10c). In general, the adsorption of oxygen molecules onto the surfaces of oxide semiconductors is a chemisorptive behaviour at elevated temperatures. Therefore, a high operating temperature is usually necessary to obtain the oxide-based gas sensors with satisfactory gas-sensing performance [28]. During this sensing process, UV light irradiation activates the electron–hole separation instead of heating activation under heating conditions, which not only decreases power consumption but also increases safety to avoid igniting inflammable and explosive gases.

4. Conclusion: A single-sheet PSC ZnO nanosheet-based gas sensor has been fabricated, which exhibited good responses to 1–300 ppm of ethanol under UV light at room temperature. The UV-activation sensing mechanism of the sensor is proposed,

which suggests a promising method for fabricated gas sensors working at room temperature.

5. Acknowledgments: This work was supported by the National Basic Research Program of China (grant no. 2013CB934304) and the National Natural Science Foundation of China (grant nos. 61673367, 61374017, 61573334 and 31571567).

6 References

- [1] Tomchenko A.A., Harmer G.P., Marquis B.T., *ET AL.*: ‘Semiconducting metal oxide sensor array for the selective detection of combustion gases’, *Sens. Actuators B, Chem.*, 2003, **93**, (1–3), pp. 126–134
- [2] Huang X., Wang L., Sun Y., *ET AL.*: ‘Quantitative analysis of pesticide residue based on the dynamic response of a single SnO₂ gas sensor’, *Sens. Actuators B, Chem.*, 2004, **99**, (2–3), pp. 330–335
- [3] Meng F.L., Li H.H., Kong L.T., *ET AL.*: ‘Parts per billion-level detection of benzene using SnO₂/graphene nanocomposite composed of sub-6 nm SnO₂ nanoparticles’, *Anal. Chim. Acta*, 2012, **736**, pp. 100–107
- [4] Sun Y., Huang X., Meng F., *ET AL.*: ‘Study of influencing factors of dynamic measurements based on SnO₂ gas sensor’, *Sensors (Basel)*, 2004, **4**, pp. 95–104
- [5] Lee J.-H.: ‘Gas sensors using hierarchical and hollow oxide nanostructures: overview’, *Sens. Actuators B, Chem.*, 2009, **140**, (1), pp. 319–336
- [6] Lu G., Xu J., Sun J., *ET AL.*: ‘UV-enhanced room temperature NO₂ sensor using ZnO nanorods modified with SnO₂ nanoparticles’, *Sens. Actuators B, Chem.*, 2012, **162**, (1), pp. 82–88
- [7] Gu C., Shanshan L., Huang J., *ET AL.*: ‘Preferential growth of long ZnO nanowires and its application in gas sensor’, *Sens. Actuators B, Chem.*, 2013, **177**, pp. 453–459
- [8] Zhang S.-L., Lim J.-O., Huh J.-S., *ET AL.*: ‘Two-step fabrication of ZnO nanosheets for high-performance VOCs gas sensor’, *Curr. Appl. Phys.*, 2013, **13**, pp. S156–S161
- [9] Meng F.L., Ge S., Jia Y., *ET AL.*: ‘Interlaced nanoflake-assembled flower-like hierarchical ZnO microspheres prepared by bisolvents and their sensing properties to ethanol’, *J. Alloys Compd.*, 2015, **632**, pp. 645–650
- [10] Meng F.L., Guo Z., Huang X.J.: ‘Graphene-based hybrids for chemiresistive gas sensors’, *TRAC Trends Anal. Chem.*, 2015, **68**, pp. 37–47
- [11] Meng F.L., Hou N.N., Jin Z., *ET AL.*: ‘Sub-PPB detection of acetone using Au-modified flower-like hierarchical ZnO structures’, *Sens. Actuators B, Chem.*, 2015, **219**, pp. 209–217
- [12] Liang Y.C., Cheng Y.R.: ‘Combinational physical synthesis methodology and crystal features correlated with oxidizing gas detection ability of one-dimensional ZnO-VO_x crystalline hybrids’, *CrystEngComm*, 2015, **17**, (30), pp. 5801–5807
- [13] Liang Y.C., Lin T.Y., Lee C.M.: ‘Crystal growth and shell layer crystal feature-dependent sensing and photoactivity performance of zinc oxide-indium oxide core-shell nanorod heterostructures’, *CrystEngComm*, 2015, **17**, (41), pp. 7948–7955
- [14] Liang Y.C., Lin T.Y.: ‘Fabrication and sensing behavior of one-dimensional ZnO–Zn₂GeO₄ heterostructures’, *Nanoscale Res. Lett.*, 2014, **9**, p. 334
- [15] Liang Y.C., Liu S.L., Hsia H.Y.: ‘Physical synthesis methodology and enhanced gas sensing and photoelectrochemical performance of 1D serrated zinc oxide-zinc ferrite nanocomposites’, *Nanoscale Res. Lett.*, 2015, **10**, p. 350
- [16] Liang Y.C., Liao W.K., Deng X.S.: ‘Synthesis and substantially enhanced gas sensing sensitivity of homogeneously nanoscale Pd- and Au-particle decorated ZnO nanostructures’, *J. Alloys Compd.*, 2014, **599**, pp. 87–92

- [17] Zhang J., Liu X.H., Neri G., *ET AL.*: 'Nanostructured materials for room-temperature gas sensors', *Adv. Mater.*, 2016, 28, 5, pp. 795–831
- [18] Guo J., Zhang J., Gong H.B., *ET AL.*: 'Au nanoparticle-functionalized 3D SnO₂ microstructures for high performance gas sensor', *Sens. Actuators B, Chem.*, 2016, 226, pp. 266–272
- [19] Kuang Q., Lao C.-S., Li Z., *ET AL.*: 'Enhancing the photon- and gas-sensing properties of a single SnO₂ nanowire based nanodevice by nanoparticle surface functionalization', *J. Phys. Chem. C*, 2008, 112, pp. 11539–11544
- [20] Fan S.-W., Srivastava A.K., Dravid V.P.: 'UV-activated room-temperature gas sensing mechanism of polycrystalline ZnO', *Appl. Phys. Lett.*, 2009, 95, (14), pp. 142106
- [21] Gong J., Li Y., Chai X., *ET AL.*: 'UV-light-activated ZnO fibers for organic gas sensing at room temperature', *J. Phys. Chem. C*, 2010, 114, pp. 1293–1298
- [22] Park S., An S., Mun Y., *ET AL.*: 'UV-enhanced NO₂ gas sensing properties of SnO₂-core/ZnO-shell nanowires at room temperature', *ACS Appl. Mater. Interfaces*, 2013, 5, (10), pp. 4285–4292
- [23] Liu J., Guo Z., Meng F., *ET AL.*: 'Novel porous single-crystalline ZnO nanosheets fabricated by annealing ZnS(en)0.5 (en=ethylenediamine) precursor. Application in a gas sensor for indoor air contaminant detection', *Nanotechnology*, 2009, 20, (12), p. 125501
- [24] Liang Y.C., Lung T.W., Wang C.C.: 'Visible photoassisted room-temperature oxidizing gas-sensing behavior of Sn₂S₃ semiconductor sheets through facile thermal annealing', *Nanoscale Res. Lett.*, 2016, 11, p. 505
- [25] Li Z.J., Lin Z.J., Wang N.N., *ET AL.*: 'High precision NH₃ sensing using network nano-sheet Co₃O₄ arrays based sensor at room temperature', *Sens. Actuators B, Chem.*, 2016, 235, pp. 222–231
- [26] Jin Z., Zhang Y.-X., Meng F.-L., *ET AL.*: 'Facile synthesis of porous single crystalline ZnO nanoplates and their application in photocatalytic reduction of Cr(VI) in the presence of phenol', *J. Hazardous Mater.*, 2014, 276, pp. 400–407
- [27] Meng F.L., Hou N.N., Jin Z., *ET AL.*: 'Ag-decorated ultra-thin porous single-crystalline ZnO nanosheets prepared by sunlight induced solvent reduction and their highly sensitive detection of ethanol', *Sens. Actuators B, Chem.*, 2015, 209, pp. 975–982
- [28] Liang Y.C., Lee C.M., Lo Y.J.: 'Reducing gas-sensing performance of Ce-doped SnO₂ thin films through a cosputtering method', *RSC Adv.*, 2014, 7, (8), pp. 4724–4734